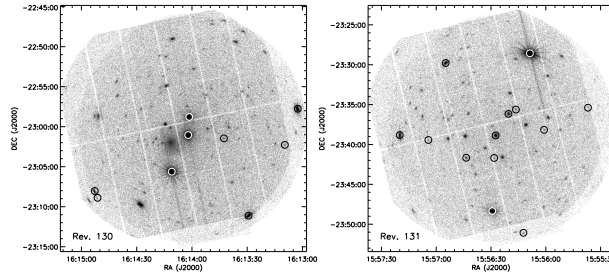


Abstract

The 5 Myr old Upper Scorpius Association, due to its vicinity (145 pc) and low circumstellar extinction, allows to perform detailed study of the X-ray emission from PMS stars. We present the results of the analysis of *XMM-Newton* observations of two Upper Scorpius regions. We detected 224 X-ray sources among which we identified 22 Upper Scorpius probable members on the basis of the 2MASS photometry. The selected Upper Scorpius sample includes 7 WTTS and 1 CTTS, while the nature of the remaining sources is not known. The analysis of the *XMM-Newton*/EPIC spectra indicates metal depleted plasma with temperature of ~ 10 MK, resembling the typical coronal emission of active main sequence stars. All the Upper Scorpius detected stars display X-ray emission near the saturation level. The Kolmogorov-Smirnov test proves that 59% of the detected X-ray Upper Scorpius sources are variable during the observations. Analysis of strong flares allows us to derive the dimensions of the coronal structures where the flares occurred.

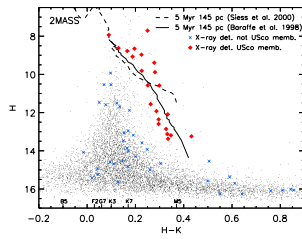
XMM Observations



XMM-Newton observed two fields of the Upper Scorpius (USco) region on 2000 August 24 and 26, with exposures of ~ 53 and ~ 43 ks. We performed X-ray source detection on a composite count rate image, obtained by the superposition of the three EPIC instruments, applying the Wavelet Transform detection algorithm (Damiani et al. 1997a,b). In the two plots on the left we show the combined EPIC images. We detected 117 and 107 sources in the two fields, having adopted threshold levels such that we expect 1 spurious source per field. A galaxy cluster is clearly visible near the center of the Rev. 130 field of view.

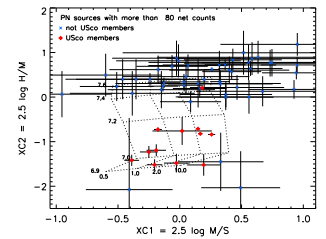
Upper Scorpius Members

Source identification was based on the 2MASS catalogue. We adopted $5''$ as matching radius between X-ray and infrared positions. We found counterparts for 60 X-ray sources (only one source has two counterparts). 22 sources, among the 224 detected, have 2MASS photometry consistent with USco membership (these 22 sources are marked with circles in the *XMM* field of view images). In the color magnitude diagram, plotted on the right, we report the position of the 22 selected stars were already known to be members of USco. We note that the Rev. 131 *XMM-Newton* field was observed also with *ROSAT*, and only 6 of the 13 USco members of this field were detected in the *ROSAT* data (Sciortino et al. 1998). There exist three known USco members not X-ray detected in the analyzed *XMM-Newton* fields; for these sources we estimated the L_X upper limits.



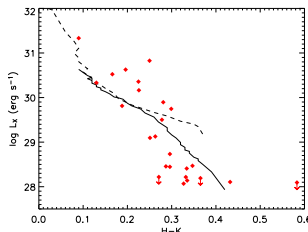
X-ray Colors

We evaluated the background subtracted number of photons in the soft (0.3 – 0.85 keV), medium (0.85 – 1.4 keV) and hard (1.4 – 7.9 keV) energy bands, indicating them with S , M and H . The plot on the right shows the X-ray colors for the strongest PN sources (net counts > 80). We compared the observed values with predictions based on typical 2- T coronal models (dotted grid). These predicted values are estimated assuming $N_H = 1.5 \times 10^{21} \text{ cm}^{-2}$, $\text{Fe}/\text{Fe}_\odot = 0.15$, $\log T_1(\text{K}) = 6.4$, $\log T_2$ spanning the range indicated on the left part of the grid, and EM_2/EM_1 ratio as indicated in the lower part of the grid. USco photometric members display $XC2$ colors significantly lower than those of non members. This plot hints on how X-ray colors may discriminate stellar coronal emission from background sources.



X-ray Spectra and Luminosities

We have analyzed the X-ray spectra of USco sources with more than 200 PN counts, adopting an absorbed 1-, 2-, 3- T isothermal plasma. Best fit models, obtained from all the EPIC instruments, indicate low extinction ($N_H \sim 0.32 - 2.38 \times 10^{21} \text{ cm}^{-2}$), low plasma metallicity ($\text{Fe} \sim 0.01 - 0.38 \text{ Fe}_\odot$), and temperature ranging from 3 to 80 MK. We estimated X-ray luminosities, in the 0.5 – 8.0 keV band from the best fit models. For USco members with low statistics, L_X values were estimated converting the PN count rate into flux adopting a conversion factor of $2.86 \times 10^{-12} \text{ erg cm}^{-2} \text{ ct}^{-1} \text{ s}^{-1}$. The plot on the right shows L_X vs. $H-K$ color. The solid and dashed lines represent the saturation levels ($\log L_X/L_{\text{bol}} = -3$) based on L_{bol} predicted by the models of Baraffe et al. (1998) and Siess et al. (2000), respectively. All the stars have X-ray emission near the saturation level.

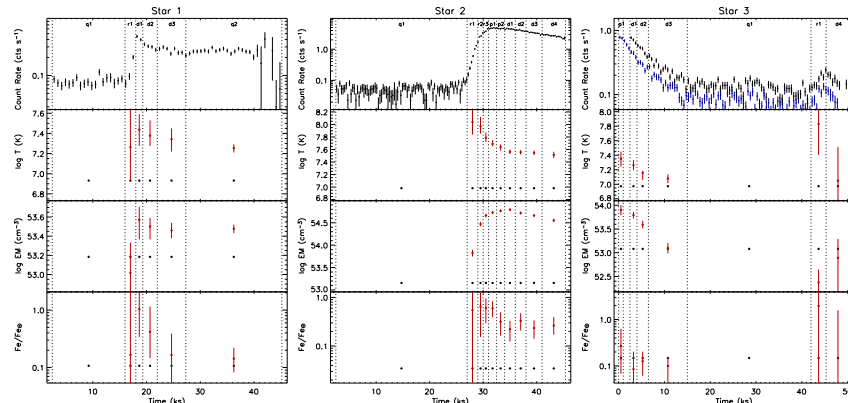


Variability

We studied the X-ray variability of all the detected sources applying the unbinned Kolmogorov-Smirnov test. We analyzed the photon events adding the PN, MOS1 and MOS2 data (and performing the intersection of GTI intervals of the three instruments). The Kolmogorov-Smirnov test was applied also to background events of each source, in order to check variability due to the background. We explored the confidence levels of 90 and 99% for testing the hypothesis of constant emission. In the Table on the right we report the results obtained for the sample of all detected X-ray sources, and for the selected subset of USco photometric members. We obtained that 13 (59%) USco X-ray sources were variable during the observation. We note these 13 sources are also those with the highest S/N among the USco photometric members.

Conf. Lev.	All Sources		USco Members	
	N_{var}	$N_{\text{var}}/N_{\text{tot}}$	N_{var}	$N_{\text{var}}/N_{\text{tot}}$
90%	43	19.2%	14	63.6%
99%	20	8.9%	13	59.1%

Individual Flare Analysis



Three sources showed intense and isolated flares (see PN light curves in the upper panels on the left). We analyzed these three flares following the Reale et al. (1997) method in order to estimate the length of the flaring structures. Note that we also plotted the MOS light curve in blue for the star 3 since the PN missed the flare peak. For each source we divided the observation in several intervals which probe the quiescent, rising, and decaying phases. The PN spectrum of each phase was fitted to derive the plasma properties. The best fit model of the quiescent phase was included in the fitting models of the flaring phases with the aim to distinguish flaring emission. The results are reported in the lower panels of the plots (black symbols mark the quiescent emission and red symbols the flaring one). The derived lengths for the flaring loops of these three stars are reported in the Table below. In all cases we found that the flaring loops have $L \leq R_*$. For star 2 and 3, we found that sustained heating was present during the decaying phases. The initial decay phases (d1, d2 and d3 intervals) of the flare of star 1 do not suggest the presence of sustained heating, however the constant and intense emission showed after the decay (q2 interval) may indicate that sustained heating occurred in this latter phase.

Star	V	$B-V$	H	$H-K$	R_*	L
					(R_\odot)	(10^{10} cm) (R_\odot)
1	13.01 ^a	1.47 ^a	8.97	0.23	2.3 ^b	11 1.6
2	8.63 ^c	0.23 ^c	7.93	0.09	$\sim 3^d$	8.7 1.2
3	9.81	0.23	$\sim 1^e$	0.94 0.13

^a From Walter et al. (1994). ^b From Adams et al. (1998). ^c From Slawson et al. (1992). ^d Estimated from the $B-V$ color and the Siess et al. (2000) models. ^e Estimated from the $H-K$ color and the Siess et al. (2000) models.

Note that the high S/N spectra allowed us to check the metallicity variations during the flares. Stars 1 and 2 showed clear evidence for higher metallicity during the flare with respect to the quiescent emission, suggesting that quiescent coronal plasma is metal depleted with respect photospheric material, which evaporates and fills the flaring loop during intense flares, provoking therefore an increment of the metallicity.

References

Adams, N. R., Walter, F. M., & Wolk, S. J. 1998, *AJ*, 116, 237
Baraffe, I., Chabrier, G., Allard, F., & Hauschildt, P. H. 1998, *A&A*, 337, 403
Damiani, F., Maggio, A., Micela, G., & Sciortino, S. 1997a, *ApJ*, 483, 350

Damiani, F., Maggio, A., Micela, G., & Sciortino, S. 1997b, *ApJ*, 483, 370
Reale, F., Betta, R., Peres, G., Serio, S., & McTiernan, J. 1997, *A&A*, 325, 782
Sciortino, S., Damiani, F., Favata, F., & Micela, G. 1998, *A&A*, 332, 825

Siess, L., Dufour, E., & Forestini, M. 2000, *A&A*, 358, 593
Slawson, R. W., Hill, R. J., & Landstreet, J. D. 1992, *ApJS*, 82, 117
Walter, F. M., Vrba, F. J., Mathieu, R. D., Brown, A., & Myers, P. C. 1994, *AJ*, 107, 692